

Article

Effects of Moss Overlay on Soil Patch Infiltration and Runoff in Karst Rocky Desertification Slope Land

Na Tu ^{1,2}, Quanhou Dai ^{1,2,*}, Youjin Yan ^{1,2}, Xudong Peng ^{1,2}, Wenping Meng ^{1,2,3} and Longpei Cen ^{1,2}¹ College of Forestry, Guizhou University, Guiyang 550025, China² Institute of Soil Erosion and Ecological Restoration, Guizhou University, Guiyang 550025, China³ Guizhou Botanical Garden, Guiyang 550025, China

* Correspondence: qhdairiver@163.com or gzudjj@163.com; Tel.: +86-137-6506-7510

Abstract: The growth and overlay of a large number of bryophytes in the broken soil patches between the exposed bedrocks of karst have an essential influence on the infiltration and runoff process between the exposed bedrocks and even the whole rocky desertification area. The purpose of this study is to explore the effects of moss on the infiltration and runoff of soil patches between karst exposed bedrocks and the processes of rainfall, runoff and infiltration transformation on slopes through rainfall experiments. The results showed that the slopes between the karst outcrops are dominated by subsurface and underground pore runoff. More than 50% of precipitation is lost through underground pores, with surface runoff accounting for only 1–17% of the total. Bryophyte overlay significantly reduced the initial runoff from subsurface and underground pore runoff, and advanced the steady-state time of runoff from subsurface and underground pore runoff, suggesting that bryophyte coverage may reduce the risk of soil erosion caused by short-duration rainfall. *Eurohypnum* has a significant inhibitory effect on percolation between exposed bedrock and reduces rainfall leakage from subsurface and underground pores. *Thuidium* has a strong intercepting effect on rainfall, significantly reducing the formation of surface runoff and the risk of surface soil erosion. Moss overlay has an essential role in soil and water conservation between karst exposed bedrock, and *Eurohypnum* and *Thuidium* can be considered as pioneer mosses for ecological restoration in the process of rocky desertification control and ecological restoration, which can effectively solve the serious problem of soil and water loss in karst rocky desertification area and improve the benefit of soil and water conservation in karst area.

Citation: Tu, N.; Dai, Q.; Yan, Y.; Peng, X.; Meng, W.; Cen, L. Effects of Moss Overlay on Soil Patch Infiltration and Runoff in Karst Rocky Desertification Slope Land. *Water* **2022**, *14*, 3429. <https://doi.org/10.3390/w14213429>

Academic Editor: Domenico Cicchella

Received: 6 October 2022

Accepted: 25 October 2022

Published: 28 October 2022

Publisher's Note: MDPI stays neutral with regard to jurisdictional claims in published maps and institutional affiliations.



Copyright: © 2022 by the authors. Licensee MDPI, Basel, Switzerland. This article is an open access article distributed under the terms and conditions of the Creative Commons Attribution (CC BY) license (<http://creativecommons.org/licenses/by/4.0/>).

Keywords: karst rocky desertification; moss coverage; exposed bedrock; soil patch rainfall infiltration

1. Introduction

Rocky desertification is one of the major ecological and environmental problems in Southwest China. It threatens the security of the local ecological environment, restricts social and economic development and has a serious impact on human life [1–4]. Soil erosion control is key to controlling rocky desertification. Therefore, how to effectively control soil erosion in rocky desert slopes has become a focus of ecological management and research in this region.

The peculiar surface–subsurface “binary three-dimensional” hydrological structure of the karst rocky desertification region has resulted in severe surface erosion and subsurface leakage [5,6]. Under this condition, the driving force of abundant precipitation causes a great loss of surface soil [3,7], resulting in the rocky desertification of karst land, simplification of vegetation structure and a large area of bare bedrock [8,9]. Therefore, the slope is cut into numerous soil patches by a large amount of exposed bedrock (Figure 1). At the same time, exposed bedrock collects large amounts of rainfall, creating a concentrated flow that directly scours and destroys soil patches. As a result, the soil patches between

these exposed bedrocks face a higher serious risk of soil erosion, which further aggravates the rocky desertification [10]. Therefore, additional studies of karst-slope soil patches are necessary.

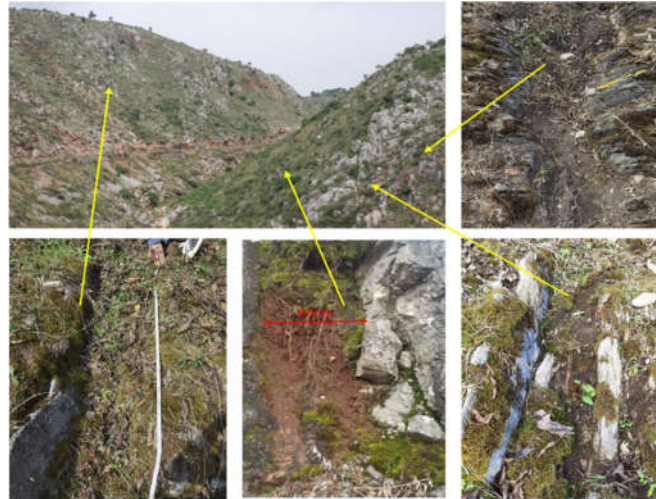


Figure 1. Soil patches between exposed bedrock on a karst rocky desertification slope.

Due to the large exposed bedrock, thin and discontinuous soil layer and serious soil degradation [11,12], most of the higher vascular plants in rocky desertification slope (especially serious rocky desertification slope) have poor recovery effect, and it is difficult to form an effective protective effect on the soil between bedrock. Bryophytes are the most typical pioneer plants in degraded ecosystems. They can not only adapt to various degraded habitats [13,14], but also are one of the most common surface cover plants on karst rocky desertification slopes [15]. Southwestern karst region, with abundant rainfall, sunshine, complex topography, habitat diversity and species rich in bryophytes [16,17]. Bryophytes are dwarf in size, and their branches and leaves are staggered and curled, commonly forming clumps or cushion-like communities. They have the characteristics of rapid water absorption and large water storage [18], and have the functions of water conservation and soil conservation. In recent years, through long-term monitoring experiments and simulated rainfall scouring experiments, it has been found that bryophytes cover the soil surface and play an influential role in intercepting rainfall, affecting soil evaporation, infiltration, runoff and other hydrological processes [19–21], thus affecting soil erosion [4,22,23].

The survey found that bryophytes grew nicely in the soil patch the karst beds, with a coverage of more than 75%. Bryophyte coverage will inevitably affect the hydrological processes of soil patches between bedrock, and thus the processes and characteristics of soil erosion [24–26]. What then will be the effect of moss cover on the hydrological processes in the soil patches between the beds, and what controls these changes? The study of these plays an essential role in soil erosion control on rocky desert slopes. However, current studies of bryophytes in rocky desert habitats have focused on plant diversity, soil physical structure and soil nutrient changes [27–30]. There have been few studies on the effects of bryophytes on soil and water conservation on karst slopes, and even fewer on the effects of bryophytes on hydrological processes in soil patches between bedrock.

In view of the lack of these studies, this study explored the effect of different moss coverings on the hydrological processes of exposed bedrock patches in rocky desert slopes based on artificially simulated rainfall. The purpose of this study is to: (1) reveal the effect of moss overlay on the spatial distribution and runoff process of soil patches between exposed bedrocks on rocky desertification slopes; (2) reveal the influence factors of the hydrological process of exposed bedrock soil patches on a rocky desertification slope. The

results can provide an essential scientific and theoretical basis for the control of desertification and the ecological restoration of karst rocks.

2. Experimental Materials and Methods

2.1. Experimental Materials and Design

In this study, we used a rectangular soil trough to model karst exposed inter-base soil patches. The soil trough is 100 cm long, 40 cm wide and 15 cm deep. The exposed bedrock was simulated with iron sheets on either side of the soil trough, and 2 mm quartz sand combined with PVC glue was applied to the surface of the soil trough and the iron sheet to simulate the roughness of the rock surface. Circular holes with a radius of 1 cm are evenly distributed at the bottom of the soil trough to simulate subsurface pore fissures (Figure 2). The designed fissure rate is 1% and the slope is 15°, which are common for fissures and slopes in karst areas [31,32]. Rainfall intensities of 50 mm/h, 70 mm/h and 90 mm/h are common in the southwestern karst region. The experimental soil is lime soil. In this study, three dominant mosses, *Bryum*, *Eurohypnum* and *Thuidium* in the karst area were used as the research objects, and bare soil was used as the control experiment. We carried out three parallel treatments in each group, a total of 36 rainfalls.

The soil samples were collected from Gaofeng Town, Anshun City, Guizhou Province (26°22′ 03.33″ N; 106°24′50.49″ E) of limestone soil in typical karst areas, 0–30 cm surface soil, remove impurities such as animal and plant residues and large stones in soil samples, naturally dried, screened by a 5 mm sieve, bagged for later use. Bryophytes used in the study are the dominant bryophytes in areas of desertification (*Bryum*, *Eurohypnum*, *Thuidium*). Sampling of bryophytes in 10 cm × 10 cm grids with 1 cm soil thickness to ensure bryophyte and soil structural integrity. In the laboratory, weeds and stones from the bryophyte samples were removed, spread on a culture plate, and pure water was sprayed to maintain the same humidity for the simulated rainfall. The bryophytes were scanned by EPSON11000XL scanner (Figure 3). The length (L), surface area (S) and volume (V) of each bryophyte were obtained by WinRHIZO2013 root analysis system. See Table 1 for a basic overview of bryophytes.

Table 1. Basic overview of bryophytes.

Bryophyte	Life form	L (cm)	S (cm ²)	V(cm ³)
B	Cluster type	1.004 ± 1.403 b	0.614 ± 0.055 b	0.003 ± 0.00 b
E	Cross type	8.996 ± 2.527 b	1.013 ± 0.163 b	0.008 ± 0.001 b
T	Cross type	17.531 ± 9.483 a	3.518 ± 1.384 a	0.033 ± 0.014 a

Note: B is *Bryum*; E is *Eurohypnum*; T is *Thuidium*; L is the length per plant of bryophytes, S is the surface area per plant of bryophytes, and V is the volume per plant of bryophytes. Lowercase letters indicate significant differences between different bryophytes ($p < 0.05$).



Figure 2. Experimental design of a soil patch device between exposed bedrock.

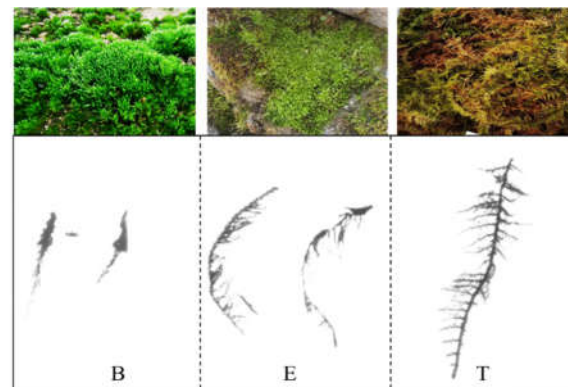


Figure 3. Field growth status and individual scans of bryophytes. Note: B is Bryum; E is Eurohypnum; T is Thuidium.

2.2. Experimental Method

We conducted a rain test in July 2021 in the laboratory of Guizhou University in Guiyang City. The rainfall equipment is described by Peng Xudong et al. [6,33]. The rainfall height is 6 m, the effective rainfall area is 6.5 m × 6.5 m, and the final raindrop velocity conforms to the characteristics of natural rainfall. The uniform distribution of raindrops is up to 85 percent, and the rainfall intensity can be controlled remotely or manually between 6 mm/h and 180 mm/h.

The method involves filling the soil with the unit weight of $1.14 \text{ g} \cdot \text{cm}^{-3}$ in soil trough, and then spreading the soil-bearing bryophytes in the soil trough. The rainfall intensity (30 mm/h) is then adjusted until the underground pore begins to produce runoff, then stand for 24 h. Before the experiment started, the soil trough was covered with plastic film, the rain intensity was adjusted to the design level, and then the plastic film was removed and the rain started. Timing begins when one of the surface, subsurface or subsurface pores begins to flow. Runoff samples of surface, subsurface and underground pore are collected every 5 min and placed in graduated vats to measure slope runoff. The slope area is the sum of the projected areas of exposed bedrock and soil on either side.

2.3. Data Analysis

(1) Coefficient of runoff (C_r)

The coefficient of runoff (C_r) is the ratio of the surface, subsurface or underground pore runoff volume to the total runoff volume. C_r is calculated by Equation (1) [33]:

$$C_r = \frac{R_i}{R} \quad (1)$$

where C_r is the coefficient of runoff, R_i is the surface, subsurface or underground runoff volume (L), and R is the total runoff volume (L).

(2) Modulus of runoff (K_r)

The modulus of runoff (K_r) is the runoff volume produced per unit time per unit area. K_r is calculated by Equation (2) [33]:

$$K_r = \frac{R_i}{At} \quad (2)$$

where K_r is the modulus of runoff (L/(m²·h)), A is the slope area (m²), and t is the rainfall duration (h).

(3) Infiltration rate

Infiltration rate reflects the amount of infiltration per unit time per unit area of soil surface, average infiltration rate (λ) is calculated by Equation (3); instantaneous infiltration rate (λ_i) is calculated by Equation (4) [34]:

$$\lambda = \frac{q \cos \alpha - R_s}{t} \quad (3)$$

$$\lambda_i = P \cos \alpha - \frac{10R_s}{(t_{i+1} - t_i)A} \quad (4)$$

where λ is the average surface infiltration rate (mm·min⁻¹); q is rainfall (mm); R_s is the surface runoff (ml); α is the slope (°); t is rainfall time (min); λ_i is the slope instantaneous infiltration rate (mm·min⁻¹); P is the rain intensity (mm·min⁻¹); A is slope projection area (cm²); t_{i+1} and t_i are the start and end time of each time period (min).

This study used Excel2016 and SPSS19.0 for statistical analysis of data. Principal component analysis (PCA) was used to analyze the correlation between different bryophytes and rainfall runoff and infiltration by using Origin9.1. At the same time, the correlation calorific value analysis between the characteristics of bryophytes such as length, surface area and volume and rainfall intensity, runoff and infiltration was carried out by using Origin9.1. We used Amos24.0 to analyze the structural equation model path of moss type, rainfall intensity, surface infiltration rate, surface coefficient, surface runoff modulus, surface runoff and other factors.

3. Results

3.1. Effect of Moss Cover on Spatial Distribution of Runoff

It can be seen from Figure 4 that the coverage of Sphagnum significantly increased surface runoff and inhibited underground and underground pore fissure flow. *Thuidium* coverage significantly reduces surface runoff. Not only moss cover but also rainfall intensity affected runoff yield between exposed bedrock, and runoff yield increased with the increase in rainfall intensity. The surface runoff under the coverage of *Eurohypnum* is between 2.28–5.53 L and is 4–7 times higher than that of *Bryum*, *Thuidium*, bare soil. Subsurface and underground pore runoff is formed by rainfall through infiltration, and moss cover has different effects on subsurface and subsurface pore runoff at different rainfall intensities. Under 50 mm/h rainfall intensity, moss coverage significantly increased subsurface and underground pore runoff, and the runoff was in the order of *Bryum* > *Thuidium* > *Eurohypnum* > bare land. Under 70 mm/h and 90 mm/h rainfall intensity, moss coverage significantly reduced the subsurface runoff, and under 90 mm/h rainfall intensity, the subsurface runoff was in the order of bare land > *Thuidium* > *Bryum* > *Eurohypnum*, and the difference between the four was extremely significant ($p < 0.01$). The underground

pore runoff is the loss of precipitation from the underground pore fissure through infiltration. At 70 mm/h rainfall intensity, moss coverage increases the underground pore runoff but the difference is not significant. At 90 mm/h rainfall intensity, moss coverage significantly inhibits the underground pore runoff, and the inhibition effect of the *Eurohypnum* and the *Bryum* is the most significant.

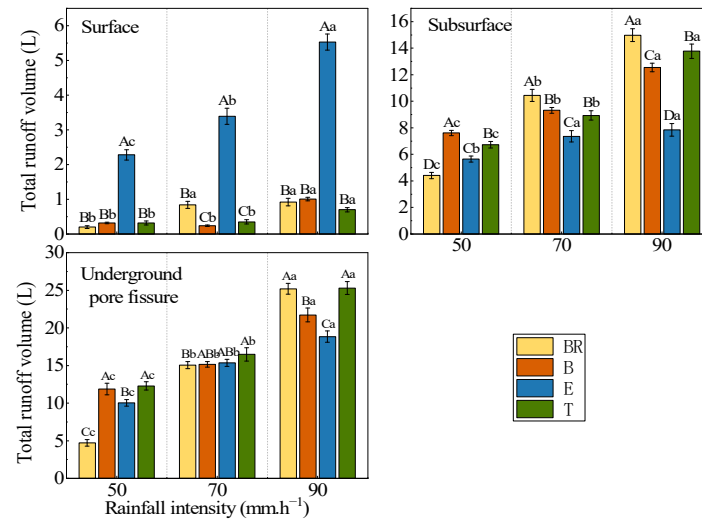


Figure 4. Effect of moss coverage on runoff yield in soil patches between exposed bedrock. Note: BR is bare land; B is *Bryum*; E is *Eurohypnum*; T is *Thuidium*; the capital letters represent the significant difference between different mosses under the same rainfall intensity and runoff type ($p < 0.05$); the lowercase letters represent the same type of mosses, under the same runoff type, the difference between different rainfall intensities is significant ($p < 0.05$).

According to Table 2, it can be seen that the coverage of *Eurohypnum* significantly increased the surface runoff coefficient, and was significantly different from the surface runoff coefficient of *Bryum*, *Thuidium* and bare land ($p < 0.01$). The underground runoff coefficient is in the order of bare land > *Bryum* > *Thuidium* > *Eurohypnum*, and the difference in the runoff coefficients between the four is extremely significant. Moss coverage significantly increased the flow coefficient of underground pores, and the flow coefficient of underground pores in the *Thuidium* genus was higher. According to Table 3, the surface runoff modulus is low, ranging from 0.31 to 8.50 L·m⁻²·h⁻¹, and the runoff modulus of *Eurohypnum* is higher and significantly different from that of bare land. The underground runoff modulus was between 6.78–23.04 L·m⁻²·h⁻¹. Bryophytes significantly increased the surface runoff modulus under 50 mm/h rainfall intensity. The runoff modulus under the coverage of *Bryum* and *Plumbago* was higher, while the moss coverage decreased the underground runoff modulus under 70 mm/h and 90 mm/h rainfall intensity. The runoff modulus of underground pore is high, and the highest runoff modulus is 38.92 L·m⁻²·h⁻¹ under 90 mm/h rainfall intensity.

Table 2. Influence of moss cover on runoff coefficient of soil between exposed bedrock patches.

Type	Rainfall Intensity (mm·h ⁻¹)	Coefficient of Runoff			
		BR	B	E	T
Surface	50	0.022 ± 0.003 Bb	0.016 ± 0.001 Bb	0.127 ± 0.004 Ab	0.016 ± 0.002 Ba
	70	0.032 ± 0.002 Ba	0.010 ± 0.001 Cc	0.130 ± 0.003 Ab	0.013 ± 0.002 Ca
	90	0.022 ± 0.002 Cb	0.029 ± 0.001 Ba	0.172 ± 0.001 Aa	0.018 ± 0.001 Da
Subsurface	50	0.473 ± 0.011 Aa	0.385 ± 0.009 Ba	0.314 ± 0.001 Da	0.348 ± 0.004 Ca
	70	0.396 ± 0.003 Ab	0.377 ± 0.006 Bb	0.282 ± 0.004 Db	0.347 ± 0.005 Ca
	90	0.365 ± 0.001 Ac	0.356 ± 0.011 ABb	0.243 ± 0.004 Dc	0.346 ± 0.002 Ca

Underground pores	50	0.505 ± 0.010 Dc	0.599 ± 0.009 Ba	0.559 ± 0.004 Cb	0.636 ± 0.003 Aa
	70	0.572 ± 0.004 Db	0.613 ± 0.007 Ba	0.588 ± 0.007 Ca	0.640 ± 0.004 Aa
	90	0.613 ± 0.002 Ba	0.616 ± 0.012 Ba	0.585 ± 0.003 Ca	0.636 ± 0.002 Aa

Note: BR is bare land; B is *Bryum*; E is *Eurohypnum*; T is *Thuidium*; the capital letters represent the significant difference between different mosses under the same rainfall intensity and runoff type ($p < 0.05$); the lowercase letters represent the same type of mosses, under the same runoff type, the difference between different rainfall intensities is significant ($p < 0.05$).

Table 3. The influence of moss cover on the runoff modulus of exposed bedrock soil patches.

Type	Rainfall Intensity (mm·h ⁻¹)	Modulus of Runoff (L/(m ² ·h))			
		BR	B	E	T
Surface	50	0.31 ± 0.06 Bcd	0.50 ± 0.04 Bb	3.51 ± 0.23 Ac	0.49 ± 0.09 Bb
	70	1.30 ± 0.15 Ba	0.37 ± 0.03 Cb	5.22 ± 0.36 Ab	0.54 ± 0.09 Cb
	90	1.41 ± 0.17 Ba	1.56 ± 0.08 Bc	8.50 ± 0.35 Aa	1.08 ± 0.09 Ba
Subsurface	50	6.78 ± 0.37 Dc	11.70 ± 0.31 Ac	8.69 ± 0.35 Cb	10.36 ± 0.38 Bc
	70	16.06 ± 0.70 Ab	14.34 ± 0.34 Bb	11.33 ± 0.64 Ca	13.74 ± 0.54 Bb
	90	23.04 ± 0.76 Aa	19.30 ± 0.49 Ca	12.07 ± 0.73 Da	21.18 ± 0.83 Ba
Underground pore fissure	50	7.25 ± 0.68 Cc	18.26 ± 1.18 Ac	15.45 ± 0.67 Bc	18.91 ± 0.85 Ac
	70	23.15 ± 0.74 Bb	23.30 ± 0.57 ABb	23.61 ± 0.73 ABb	25.36 ± 1.35 Ab
	90	38.76 ± 1.11 Aa	33.41 ± 1.40 Ba	28.98 ± 1.15 Ca	38.92 ± 1.29 Aa

Note: BR is bare land; B is *Bryum*; E is *Eurohypnum*; T is *Thuidium*; the capital letters represent the significant difference between different mosses under the same rainfall intensity and runoff type ($p < 0.05$); the lowercase letters represent the same type of mosses, under the same runoff type, the difference between different rainfall intensities is significant ($p < 0.05$).

The rainfall on the slope between karst exposed bedrock mainly forms the subsurface and underground pore runoff. As shown in Figure 5, the surface runoff ratio is small (1–17%), followed by the subsurface runoff ratio (24–47%), and the underground pore runoff ratio is the highest and higher than 50%. Under the three rainfall intensities, the surface runoff of *Eurohypnum* was relatively elevated and higher than 10%, while the surface runoff ratios of the other two bryophytes and bare land were lower than 5%. The subsurface runoff ratio of bare land is the highest under three rainfall intensities, and the runoff ratio of bare land is as high as 47% under 50 mm/h rainfall intensity. In the underground pore runoff ratio, the underground runoff ratio of *Thuidium* under three rainfall intensities was higher than that of the other two mosses and bare land, and the runoff ratio was up to 64%.

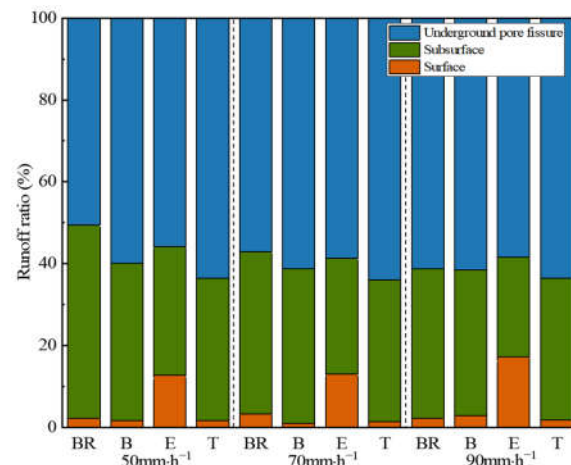


Figure 5. The effect of bryophytes on the proportion of runoff in soil patches between exposed beds. Note: BR is bare land; B is *Bryum*; E is *Eurohypnum*; T is *Thuidium*.

3.2. Effect of Moss Cover on Percolation-Runoff Process

Runoff of *Bryum*, *Eurohypnum*, *Thuidium* and bare Land vary with rainfall duration as shown in Figure 6. With the increase in rainfall intensity, the initial runoff increased and the stable time of runoff advanced. In surface runoff, *Eurohypnum* not only significantly increases surface runoff, but also lags behind the stability time of surface runoff with an average time of 45 min. The stable time of surface runoff was advanced under the coverage of *Bryum* and *Thuidium* plants. In subsurface runoff, bryophytes significantly reduce the initial subsurface runoff. Initial runoff in *Eurohypnum* and *Bryum* was low at 70 mm/h and 90 mm/h rainfall intensity, and significantly different from that of the bare land. In the underground pore runoff, the runoff yield of bryophytes increased sharply at 50 mm/h rainfall intensity, and tended to be stable after 40 min of rainfall duration, while the runoff yield of bare land increased slowly in the first 30 min and tended to be stable in 35 min. At rainfall intensities of 70 mm/h and 90 mm/h, the runoff from the underground pores increases dramatically during the first 20 min of the rainfall duration. Under the coverage of *Eurohypnum* and *Thuidium*, the runoff of underground pore first reached the stability of runoff, and the bare land and *Bryum* lagged the stability time of runoff of the underground pore. On the whole, moss coverage increased the initial surface runoff, and the initial surface runoff covered by *Eurohypnum* was higher and lagged behind the stable runoff. Moss coverage significantly reduces the initial runoff in the subsurface and underground pores and stabilizes the runoff in the subsurface and underground pores in advance.

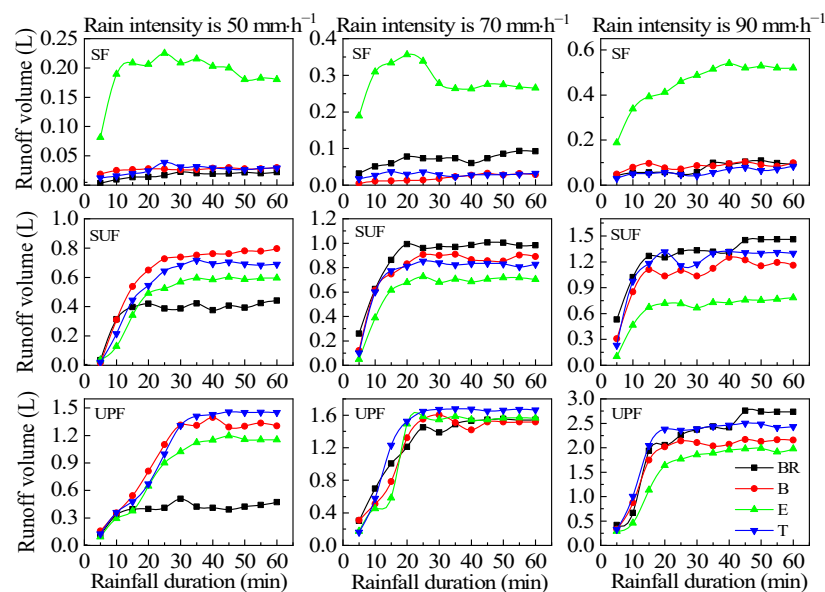


Figure 6. Variational characteristics of runoff yield for soil patches between exposed bedrock as a function of rainfall duration. Note: SF is surface; SUF is subsurface; UPF is underground pores; BR is bare land; B is *Bryum*; E is *Eurohypnum*; T is *Thuidium*.

Soil water infiltration is the process of rainfall from the soil surface into its internal movement and storage [35]. Infiltration is a direct factor in the yield of runoff. The peculiar underground “binary” structure in the karst area, the development of underground pores and fissures makes the slope rainfall infiltration swift [6]. However, rainfall infiltration is not only affected by site conditions and rainfall intensity, but also affected by moss overlay. According to Figure 7, the percolation rate increases with increasing rainfall intensity, the percolation rate is lower in the case of *Eurohypnum* plant coverage, the percolation rate changes considerably with increasing rainfall duration, and the percolation rate decreases sharply during 0–25 min of rainfall duration. The infiltration rate of bare land, *Bryum* and

Thuidium decreased gradually with the increase in rainfall duration and the overall shift of infiltration rate was not significant after 40 min of rainfall duration. In 50 mm/h rainfall intensity, the infiltration rate under moss coverage is lower than that of bare land, indicating that under low rainfall intensity, moss coverage inhibits rainfall infiltration. In the 70 mm/h rainfall intensity, *Eurohypnum* coverage promoted surface runoff and infiltration, while the infiltration under *Bryum* and *Thuidium* coverage was higher than that of bare land, and the infiltration rate was significantly different from that of bare land after the infiltration rate was stable, which proved that in the larger rainfall intensity, *Bryum* and *Thuidium* plant coverage promoted surface infiltration and inhibited surface runoff formation. In 90 mm/h rainfall intensity, the infiltration rate of bare land, *Bryum* and *Thuidium* had the same change rule in rainfall duration, and the instantaneous infiltration rate of the three was not significant, indicating that *Bryum* and *Thuidium* had no significant effect on surface infiltration and runoff at 90 mm/h rainfall intensity.

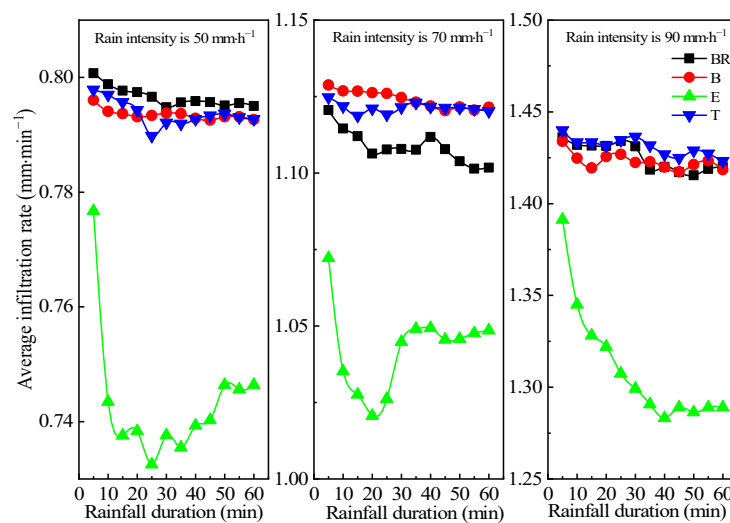


Figure 7. Variational characteristics of the surface permeability of exposed bedrock soil patches as a function of rainfall duration. Note: BR is bare land; B is *Bryum*; E is *Eurohypnum*; T is *Thuidium*.

According to Figure 8, the average infiltration rates of bare land, *Bryum* and *Thuidium* were not significantly different, and the average infiltration rates of the three were higher than that of *Eurohypnum*. The average infiltration rate of *Eurohypnum* was low, between 0.74–1.31 mm·min⁻¹. The average infiltration rate of bare land, *Bryum* and *Thuidium* was between 0.80–1.43 mm·min⁻¹. The average infiltration rate under moss coverage at 90 mm/h rainfall intensity was twice that at 50 mm/h rainfall intensity.

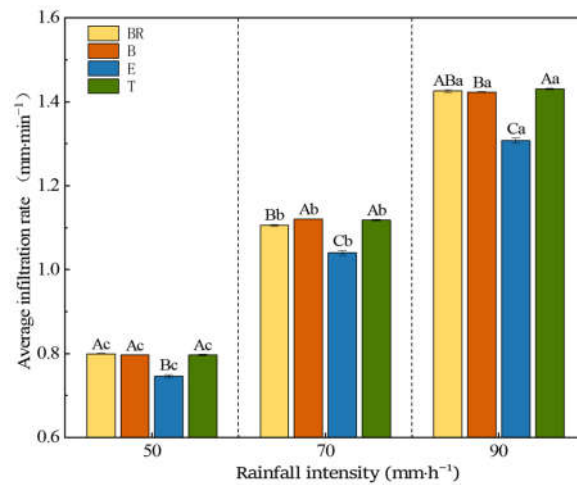


Figure 8. Effect of moss coverage on the average percolation rate of soil patches between exposed beds. Note: BR is bare land; B is *Bryum*; E is *Eurohypnum*; T is *Thuidium*. Capital letters represent the significant difference between different bryophyte genera under the same rainfall intensity ($p < 0.05$). The lowercase letters represent the same bryophyte, and the difference between different rainfall intensities is significant ($p < 0.05$).

3.3. Correlation Analysis of Moss Cover between Exposed Bedrock on Percolation-Runoff

The results of principal component analysis showed that *Eurohypnum* coverage significantly increased surface runoff, surface runoff coefficient and surface runoff modulus, while *Thuidium* coverage significantly inhibited the formation of surface runoff (Figure 9). There is a strong positive correlation between rainfall intensity and infiltration, runoff and runoff modulus.

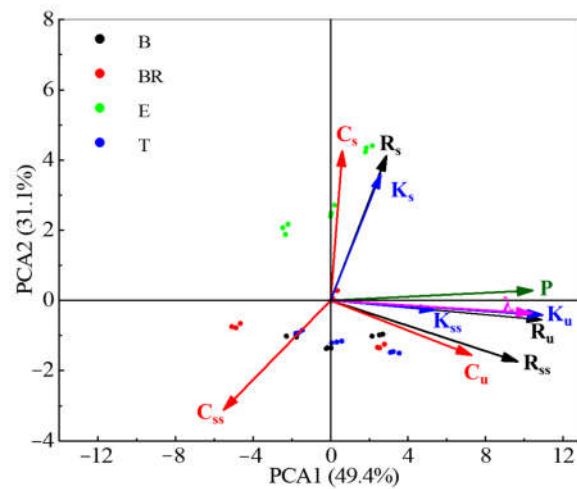


Figure 9. Principal component analysis (PCA) of different bryophytes and rainfall infiltration. Note: BR is bare land; B is *Bryum*; E is *Eurohypnum*; T is *Thuidium*. R_s is the surface runoff; R_{ss} is underground runoff; R_u is the underground pore flow; C_s is the surface runoff coefficient; C_{ss} is an underground runoff coefficient; C_u is the underground pore runoff coefficient; K_s is the surface runoff modulus; K_{ss} is an underground runoff modulus; K_u is the underground pore runoff modulus; λ is the average infiltration rate.

Different bryophytes have different morphological characteristics, plant length, surface area, volume and life forms, so the effect of different bryophytes on runoff yield on slopes between exposed beds is different. Therefore, the correlation heat map analysis of the length, surface area and volume of bryophyte plants on the inflow and infiltration of

slope under different rainfall conditions (Figure 10). The results of the correlation analysis show that the plant length of the bryophytes is positively correlated with the plant surface and volume. The plant length, surface area and volume of the bryophytes were positively correlated with the coefficient of runoff from underground pores and fissures on the slopes between exposed beds, with coefficients of 0.51, 0.71 and 0.69, respectively. The plant length, surface area, and volume of the bryophyte were negatively correlated with surface runoff, surface runoff modulus, and surface runoff coefficient.

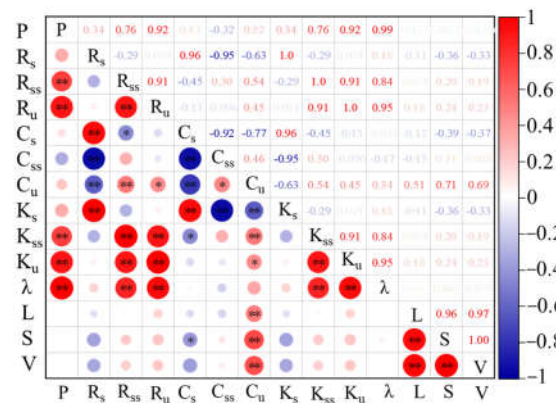


Figure 10. Heatmap of the correlation between the basic features of the bryophyte and the rainfall penetration. Note: P is the rain intensity; Rs is the surface runoff; Rss is underground runoff; Ru is the underground pore flow; Cs is the surface runoff coefficient; Css is an underground runoff coefficient; Cu is the underground pore runoff coefficient; Ks is the surface runoff modulus; Kss is an underground runoff modulus; Ku is the underground pore runoff modulus; λ is the average infiltration rate; L is the single plant length of bryophytes; S is the surface area per plant of bryophytes; V is the single plant volume of bryophytes.

The path analysis results of the structural equation model showed that the moss type and rainfall intensity jointly affected the surface infiltration rate (Figure 11), and the path determination coefficient (R^2) was 0.98, but the moss cover had a negative effect on the surface infiltration. Rainfall increased surface runoff by increasing the surface runoff modulus with a correlation factor of 0.93 and 0.96, respectively. The correlation between bryophyte types and surface runoff is not significant, and surface runoff is mainly affected by rainfall intensity and runoff molding. Bryophytes mainly inhibit percolation, thereby reducing rainfall leakage through subsurface and underground pores.

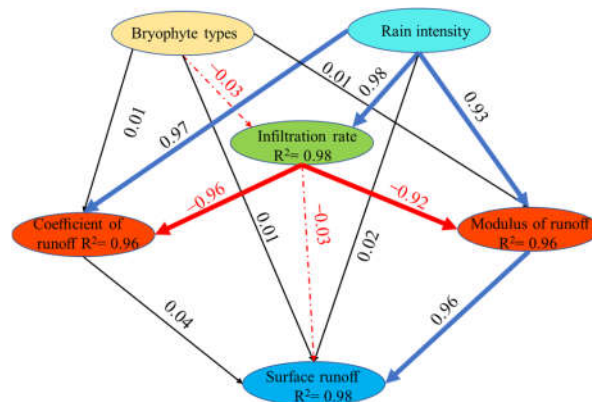


Figure 11. Model of the path structure equation for moss type and rainfall intensity on surface runoff.

4. Discuss

4.1. The Effect of Moss Overlay on the Spatial Distribution of Slope Runoff between Exposed Bedrocks

In this study, most of the rainfall between exposed bedrock formations was subsurface and underground pore runoff, and surface runoff was minor, accounting for less than 20% of the total. This is because the exposed bedrock and soil form a rock–soil interface [36–38], and the rock and soil cannot be sufficiently adhered together, typically forming a narrow gap. During the rainfall process, the production flows through these narrow gaps to form a preferential flow [39], so that the rainfall quickly infiltrates into the lower soil layer, forming subsurface runoff and underground pore fissure runoff [40–43]. Rainfall is one of the land water sources, and rainfall intensity is the main factor affecting runoff [44,45]. Under certain conditions, the greater the intensity of the rainfall, the greater the amount of rainfall and the greater the slope runoff [21,46]. Dandan Han et al. found a positive correlation between rainfall intensity and slope runoff, as well as delayed vegetation cover and reduced slope runoff [47]. This study found that the surface runoff yield of bare land was lower at 50 mm/h rainfall intensity, while the surface runoff yield of bare land was higher than that of *Thuidium* at 70 and 90 mm/h rainfall intensities. It is because the coverage of bryophytes reduces the evaporation of some soil moisture [19,20]. In addition, the total runoff yield is lower at low rainfall intensities, and bare land absorbs some of the rainfall, resulting in a lower runoff yield at low rainfall intensities for bare land. Under extreme rainfall intensity, heavy rainfall makes bare land quickly form runoff [48], and bryophytes have strong water holding capacity [49–51], so that some bryophytes reduce runoff formation.

Rainfall is the fundamental source of runoff on the slopes, and rainfall intensity is strongly positively correlated with runoff yield, runoff modulus and runoff coefficient [33]. Surface cover is one of the factors that shift the spatial distribution of runoff. The length, surface area and life form of different bryophytes are different, which affect the surface, subsurface and underground pore runoff. The study showed that the surface area and volume of bryophytes were positively correlated with the runoff yield, runoff modulus, and infiltration rate of subsurface and subsurface pores between exposed bedrocks (Figure 10). This is because bryophytes with large surface area and volume reduce the ability of rainfall to erode and splash surface soil, intercepting a portion of the rainfall, reducing the formation of surface runoff and preventing soil erosion.

4.2. The Effect of Moss Coverage on the Runoff Process between Exposed Bedrock Slopes

In this study, the effect of rainfall intensity on slope runoff was significant, and the growth overlay of bryophytes redistributed the rainfall between the exposed bedrocks in the karst rocky desertification area [24]. Ground cover plants such as mosses and algae are one of the main factors affecting runoff. In this study, runoff increased and eventually stabilized as the duration of rainfall increased. With the increase in rainfall intensity, the initial runoff increased [52], and the stability time of runoff lagged behind. Runoff between exposed bedrock increases rapidly during the first 20 min of the rainfall process. Yan Youjin [33] and Xia Zhang [53] found that the runoff increased rapidly during the rainfall process after the rainfall formed runoff. When percolation is stable, surface, subsurface and underground pore runoff tend to be stable. The stability of rainfall runoff is also affected by the surface cover. A large number of studies have shown that the interception effect of broad-leaved is stronger than that of coniferous, and the surface runoff is higher under the coverage of coniferous litter [54,55]. In this study, *Thuidium* plants reduced surface runoff and reduced the risk of surface soil erosion to a certain extent. *Eurohypnum* plants have a significant hysteresis effect on the stability of surface runoff, allowing soil infiltration to be moderate under moss cover and reducing subsurface and underground pore water loss. In the process of rainfall, the runoff of subsurface and underground pore fissures will increase rapidly with the increase in rainfall duration, and then

tend to be stable, which is consistent with the research results of Peng Xudong et al. [31]. This suggests that the increased duration of rainfall not only increases surface erosion, but also causes severe seepage from subsurface and underground pores, which exacerbates the occurrence of heavy rock desertification.

The rainfall infiltration rate is not only affected by rainfall intensity, but also shows different rules under different surface cover. Bryophyte growth coverage significantly affects soil physical and chemical properties [27], surface roughness [56,57] and soil permeability [58], thereby promoting or inhibiting slope runoff to varying degrees. In this study, the *Eurohypnum* plant had a strong inhibitory effect on surface percolation. As the intensity of rainfall increases, the rate of percolation under moss cover increases significantly. The reason is that at low rainfall intensities, the secretions of bryophytes bind to the soil, blocking soil capillary pores and preventing soil water infiltration, thus reducing the infiltration rate [30,59,60]. Larger rainfall intensities produce larger surface runoff, which disrupts the crust formed by moss secretions and soil, thus creating excellent infiltration channels on the surface and underground and accelerating rainfall penetration [30].

Eurohypnum plants are cylindrical in diameter, with fewer branches and narrow leaves [61]. They are interwoven and creeping, forming an excellent interception layer on the surface. Lengthy, cylindrical plants grow along the slopes, providing a great diversion for surface runoff. Moreover, the *Eurohypnum* plant has a strong water holding capacity [61]. In the process of rainfall settlement, the moss plants absorb part of the water, thereby reducing the infiltration of rainfall. Bryophytes and *Thuidium* plants significantly increase runoff from subsurface and underground pores, as Bryophytes grow in clumps, have dense clumps of roots and are firmly earth-fixing, thus allowing Bryophytes and soil to form a thicker crust, which with water evaporation shrinks, thus creating discontinuous surface cracks in the crust [52,62,63]. Runoff seeps through crevices and forms subsurface and underground pore flows during rainfall [6,32]. *Thuidium* plants have additional branches, longer plants, larger surface area and volume, so that the mosses in the unit area form a thicker interwoven creeping cushion, and that rainfall can produce surface runoff lag, increase rainfall infiltration and reduce the formation of surface runoff. *Eurohypnum* plants inhibit underground runoff, thereby reducing the loss of underground water and soil resources. *Thuidium* plants have an intercepting effect on surface runoff and inhibit the formation of surface runoff, which can effectively reduce surface soil erosion in karst areas.

5. Conclusions

There is significant subsurface leakage of rainwater between the exposed bedrock of the karst. More than 50% of the precipitation is lost from the cracks of underground pore, and the surface runoff is only 1–17% of the total runoff. Bryophyte coverage significantly reduces the initial runoff from subsurface and underground pores, and stabilizes the runoff from subsurface and underground pores in advance. The surface infiltration rate under *Eurohypnum* coverage was 6–8% lower than that of bare land. *Eurohypnum* significantly reduced precipitation infiltration and reduced the loss of water resources in the subsurface and underground pores. *Thuidium* coverage reduces surface runoff and the risk of surface rainfall erosion. Therefore, it can be considered as the pioneer moss of ecological restoration between exposed bedrocks in karst areas. The coverage area of *Eurohypnum* and *Thuidium* can be increased by in situ protection or artificial planting, which can effectively solve the serious problem of soil erosion between exposed bedrocks in karst areas and improve the soil and water conservation benefits in karst areas.

Author Contributions: N.T. and Q.D. contributed to the conception of the study; N.T., L.C. and W.M. performed the experiment; N.T. and Q.D., contributed significantly to analysis and manuscript preparation; N.T. and Y.Y. performed the data analyses and wrote the manuscript; N.T., X.P., Y.Y. and Q.D. helped perform the analysis with constructive discussions. All authors have read and agreed to the published version of the manuscript.

Funding: This research was funded by Natural Science Foundation of China (42167044, 42007054), China Postdoctoral Science Foundation (2020M673296), the High-level Innovative Talents in Guizhou Province of Guizhou Province (Qian Ke He Platform Talents (2018)5641), the Guizhou Province Graduate Research Fund (YJSCXJH [2020]065, YJSCXJH [2020]066), the first-class discipline Construction Project of Guizhou Province (GNYL (2017)007), and Basic Research Project of Guizhou Province [2020]1Y074.

Data Availability Statement: The data presented in this study are available on request from the corresponding author.

Conflicts of Interest: All authors declare that they have no conflict of interest in this work. We declare that we do not have any commercial or associative interest that represents a conflict of interest in connection with the work submitted.

References

1. Wang, S.-J.; Liu, Q.-M.; Zhang, D.-F. Karst Rocky Desertification in Southwestern China: Geomorphology, Landuse, Impact and Rehabilitation. *Land Degrad.* **2004**, *7*, 115–121. <https://doi.org/10.1002/ldr.592>.
2. Li, Y.; Shao, J.; Yang, H.; Bai, X. The Relations between Land Use and Karst Rocky Desertification in a Typical Karst Area, China. *Environ. Geol.* **2009**, *57*, 621–627. <https://doi.org/10.1007/s00254-008-1331-z>.
3. Zhou, L. The Challenge of Soil Loss Control and Vegetation Restoration in the Karst Area of Southwestern China. *Int. Soil Water Conserv. Res.* **2020**, *9*, 26–34. <https://doi.org/10.1016/j.iswcr.2019.12.001>.
4. Jiang, Z.; Lian, Y.; Qin, X. Rocky Desertification in Southwest China: Impacts, Causes, and Restoration. *Earth Sci. Rev.* **2014**, *12*, 1–12.
5. Dai, Q.; Peng, X.; Wang, P.; Li, C.; Shao, H. Surface Erosion and Underground Leakage of Yellow Soil on Slopes in Karst Regions of Southwest China. *Land Degrad. Dev.* **2018**, *29*, 2438–2448. <https://doi.org/10.1002/ldr.2960>.
6. Peng, X. Role of Underground Fissure Flow in Near-Surface Rainfall-Runoff Process on a Rock Mantled Slope in the Karst Rocky Desertification Area. *Eng. Geol.* **2018**, *243*, 10–17. <https://doi.org/10.1016/j.enggeo.2018.06.007>.
7. Wang, J.; Zou, B.; Liu, Y.; Tang, Y.; Zhang, X.; Yang, P. Erosion-Creep-Collapse Mechanism of Underground Soil Loss for the Karst Rocky Desertification in Chenqi Village, Puding County, Guizhou, China. *Environ. Earth Sci.* **2014**, *72*, 2751–2764. <https://doi.org/10.1007/s12665-014-3182-0>.
8. Zhang, Z.; Huang, X.; Zhou, Y. Factors Influencing the Evolution of Human-driven Rocky Desertification in Karst Areas. *Land Degrad. Dev.* **2021**, *32*, 817–829. <https://doi.org/10.1002/ldr.3731>.
9. Chengfang, Li.; Zhongcheng, W.; Zhenwei, L.; Xianli, X. Soil erosion impacts on nutrient deposition in a typical karst watershed. *Agric. Ecosyst. Environ.* **2021**, *322*, 107649. <https://doi.org/10.1016/j.agee.2021.107649>.
10. Tani, M. Runoff Generation Processes Estimated from Hydrological Observations on a Steep Forested Hillslope with a Thin Soil Layer. *J. Hydrol.* **1997**, *200*, 84–109. [https://doi.org/10.1016/S0022-1694\(97\)00018-8](https://doi.org/10.1016/S0022-1694(97)00018-8).
11. Gao, J.; Wang, H. Temporal Analysis on Quantitative Attribution of Karst Soil Erosion: A Case Study of a Peak-Cluster Depression Basin in Southwest China. *CATENA* **2019**, *172*, 369–377. <https://doi.org/10.1016/j.catena.2018.08.035>.
12. Gan, F.; He, B.; Qin, Z.; Li, W. Role of Rock Dip Angle in Runoff and Soil Erosion Processes on Dip/Anti-Dip Slopes in a Karst Trough Valley. *J. Hydrol.* **2020**, *588*, 125093. <https://doi.org/10.1016/j.jhydrol.2020.125093>.
13. Yang, T.; Chen, Q.; Yang, M.; Wang, G.; Zheng, C.; Zhou, J.; Jia, M.; Peng, X. Soil Microbial Community under Bryophytes in Different Substrates and Its Potential to Degraded Karst Ecosystem Restoration. *Int. Biodeterior. Biodegrad.* **2022**, *175*, 105493. <https://doi.org/10.1016/j.ibiod.2022.105493>.
14. Zhang, X.; Zhao, Y.; Wang, S. Responses of Antioxidant Defense System of Epilithic Mosses to Drought Stress in Karst Rock Desertified Areas. *Acta Geochim.* **2017**, *36*, 205–212. <https://doi.org/10.1007/s11631-017-0140-z>.
15. *Biological Soil Crusts: Structure, Function, and Management*; Belnap, J.; Lange, O.L.; Eds.; Ecological Studies; Springer: New York, NY, USA, 2001; ISBN 9783540410751.
16. Ni, J.; Luo, D.H.; Xia, J.; Zhang, Z.H.; Hu, G. Vegetation in Karst Terrain of Southwestern China Allocates More Biomass to Roots. *Solid Earth* **2015**, *6*, 799–810. <https://doi.org/10.5194/se-6-799-2015>.
17. Wu, Z.; Behzad, H.M.; He, Q.; Wu, C.; Bai, Y.; Jiang, Y. Seasonal Transpiration Dynamics of Evergreen *Ligustrum Lucidum* Linked with Water Source and Water-Use Strategy in a Limestone Karst Area, Southwest China. *J. Hydrol.* **2021**, *12*, 126199. <https://doi.org/10.1016/j.jhydrol.2021.126199>.
18. Moor, H.; Norberg, J. Towards a Trait-based Ecology of Wetland Vegetation. *J. Ecol.* **2017**, *13*, 1623–1635. <https://doi.org/10.1111/1365-2745.12734>.
19. Li, S.; Xiao, B. Cyanobacteria and Moss Biocrusts Increase Evaporation by Regulating Surface Soil Moisture and Temperature on the Northern Loess Plateau, China. *CATENA* **2022**, *212*, 106068. <https://doi.org/10.1016/j.catena.2022.106068>.
20. Jia, R.; Li, X.; Liu, L.; Pan, Y.; Gao, Y.; Wei, Y. Effects of Sand Burial on Dew Deposition on Moss Soil Crust in a Revegetated Area of the Tennger Desert, Northern China. *J. Hydrol.* **2014**, *519*, 2341–2349. <https://doi.org/10.1016/j.jhydrol.2014.10.031>.
21. Dai, Q.; Peng, X.; Yang, Z.; Zhao, L. Runoff and Erosion Processes on Bare Slopes in the Karst Rocky Desertification Area. *CATENA* **2017**, *152*, 218–226. <https://doi.org/10.1016/j.catena.2017.01.013>.

22. Song, L.; Zhang, Y.J.; Chen, X.; Li, S.; Lu, H.-Z.; Wu, C.-S.; Tan, Z.-H.; Liu, W.-Y.; Shi, X.-M. Water Relations and Gas Exchange of Fan Bryophytes and Their Adaptations to Microhabitats in an Asian Subtropical Montane Cloud Forest. *J. Plant Res.* **2015**, *128*, 573–584. <https://doi.org/10.1007/s10265-015-0721-z>.
23. Fischer, T.; Veste, M.; Schaaf, W. Initial Pedogenesis in a Topsoil Crust 3 Years after Construction of an Artificial Catchment in Brandenburg, NE Germany. *Biogeochemistry* **2010**, *101*, 165–176. <https://doi.org/10.1007/s10533-010-9464-z>.
24. Belnap, J.; Wilcox, B.P.; Scoyoc, M.W.V.; Phillips, S.L. Successional Stage of Biological Soil Crusts: An Accurate Indicator of Ecohydrological Condition. *Ecohydrology* **2013**, *6*, 474–482. <https://doi.org/10.1002/eco.1281>.
25. Liu, D.; She, D. Combined Effects of Moss Crusts and Pine Needles on Evaporation of Carbonate-Derived Laterite from Karst Mountainous Lands. *J. Hydrol.* **2020**, *586*, 124859. <https://doi.org/10.1016/j.jhydrol.2020.124859>.
26. Zhao, L.; Liu, Y.; Wang, Z.; Yuan, S.; Qi, J.; Zhang, W.; Wang, Y.; Li, X. Bacteria and fungi differentially contribute to carbon and nitrogen cycles during biological soil crust succession in arid ecosystems. *Plant Soil* **2020**, *447*, 379–392. <https://doi.org/10.1007/s11104-019-04391-5>.
27. Zhang, Y. Soil Nutrients, Enzyme Activities, and Microbial Communities Differ among Biocrust Types and Soil Layers in a Degraded Karst Ecosystem. *CATENA*, **2022**, *212*, 106057. <https://doi.org/10.1016/j.catena.2022.106057>.
28. Cheng, C.; Li, Y.; Long, M.; Gao, M.; Zhang, Y.; Lin, J.; Li, X. Moss Biocrusts Buffer the Negative Effects of Karst Rocky Desertification on Soil Properties and Soil Microbial Richness. *Plant Soil* **2022**, *475*, 153–168. <https://doi.org/10.1007/s11104-020-04602-4>.
29. Ren, H.; Wang, F.; Ye, W.; Zhang, Q.; Han, T.; Huang, Y.; Chu, G.; Hui, D.; Guo, Q. Bryophyte Diversity Is Related to Vascular Plant Diversity and Microhabitat under Disturbance in Karst Caves. *Ecol. Indic.* **2021**, *120*, 106947. <https://doi.org/10.1016/j.ecolind.2020.106947>.
30. Chamizo, S.; Cantón, Y.; Miralles, I.; Domingo, F. Biological Soil Crust Development Affects Physicochemical Characteristics of Soil Surface in Semiarid Ecosystems. *Soil Biol. Biochem.* **2012**, *49*, 96–105. <https://doi.org/10.1016/j.soilbio.2012.02.017>.
31. Peng, X.; Dai, Q.; Ding, G.; Li, C. Role of underground leakage in soil, water and nutrient loss from a rock-mantled slope in the karst rocky desertification area. *J. Hydrol.* **2019**, *578*, 124086. <https://doi.org/10.1016/j.jhydrol.2019.124086>.
32. Dai, Q.; Peng, X.; Zhao, L.; Shao, H.; Yang, Z. Effects of Underground Pore Fissures on Soil Erosion and Sediment Yield on Karst Slopes. *Land Degrad.* **2017**, *28*, 1922–1932. <https://doi.org/10.1002/ldr.2711>.
33. Yan, Y.; Dai, Q.; Yuan, Y.; Peng, X.; Zhao, L.; Yang, J. Effects of Rainfall Intensity on Runoff and Sediment Yields on Bare Slopes in a Karst Area, SW China. *Geoderma* **2018**, *330*, 30–40. <https://doi.org/10.1016/j.geoderma.2018.05.026>.
34. Wang, Y. *Effect of Antecedent Soil Water Content on Infiltration-Runoff during Simulated Rainfall*; Graduate Institute of Chinese Academy of Sciences (Soil and Water Conservation and Ecological Environment Research Center of Ministry of Education): Yangling, China, 2016. (In Chinese)
35. Römkens, M.J.M.; Helming, K.; Prasad, S.N. Soil Erosion under Different Rainfall Intensities, Surface Roughness, and Soil Water Regimes. *CATENA* **2002**, *46*, 103–123. [https://doi.org/10.1016/S0341-8162\(01\)00161-8](https://doi.org/10.1016/S0341-8162(01)00161-8).
36. Zhang, X.; Bai, X.; He, X. Soil Creeping in the Weathering Crust of Carbonate Rocks and Underground Soil Losses in the Karst Mountain Areas of Southwest China. *Carbonates Evaporites* **2011**, *26*, 149–153. <https://doi.org/10.1007/s13146-011-0043-8>.
37. Yang, J. Saturation effects on horizontal and vertical motions in a layered soil–bedrock system due to inclined SV waves. *Soil Dyn. Earthq. Eng.* **2001**, *21*, 527–536. [https://doi.org/10.1016/S0267-7261\(01\)00015-X](https://doi.org/10.1016/S0267-7261(01)00015-X).
38. Wright, S.N.; Novakowski, K.S. Numerical Analysis of Midwinter Infiltration along the Soil-Rock Interface: A Pathway for Enhanced Bedrock Recharge. *Adv. Water Resour.* **2022**, *166*, 104261. <https://doi.org/10.1016/j.advwatres.2022.104261>.
39. Sohr, J.; Ries, F.; Sauter, M.; Lange, J. Significance of Preferential Flow at the Rock Soil Interface in a Semi-Arid Karst Environment. *CATENA* **2014**, *123*, 1–10. <https://doi.org/10.1016/j.catena.2014.07.003>.
40. Raizada, A.; Juyal, G.P. Tree Species Diversity, Species Regeneration and Biological Productivity of Seeded Acacia Catechu Willd. In Rehabilitated Limestone Mines in the North West Indian Himalayas. *Land Degrad.* **2012**, *23*, 167–174. <https://doi.org/10.1002/ldr.1067>.
41. Peng, X. Drivers of Soil Erosion and Subsurface Loss by Soil Leakage during Karst Rocky Desertification in SW China. *Int. Soil Water Conserv. Res.* **2022**, *10*, 217–227. <https://doi.org/10.1016/j.iswcr.2021.10.001>.
42. Fang, Q.; Zhao, L.; Hou, R.; Fan, C.; Zhang, J. Rainwater Transformation to Runoff and Soil Loss at the Surface and Belowground on Soil-Mantled Karst Slopes under Rainfall Simulation Experiments. *CATENA* **2022**, *215*, 106316. <https://doi.org/10.1016/j.catena.2022.106316>.
43. Peng, J.; Wang, F.; Cheng, Y.; Lu, Q. Characteristics and Mechanism of Sanyuan Ground Fissures in the Weihe Basin, China. *Eng. Geol.* **2018**, *247*, 48–57. <https://doi.org/10.1016/j.enggeo.2018.10.024>.
44. Fang, N.-F.; Shi, Z.-H.; Li, L.; Guo, Z.-L.; Liu, Q.-J.; Ai, L. The Effects of Rainfall Regimes and Land Use Changes on Runoff and Soil Loss in a Small Mountainous Watershed. *CATENA* **2012**, *99*, 1–8. <https://doi.org/10.1016/j.catena.2012.07.004>.
45. Mohamadi, M.A.; Kaviani, A. Effects of Rainfall Patterns on Runoff and Soil Erosion in Field Plots. *Int. Soil Water Conserv. Res.* **2015**, *3*, 273–281. <https://doi.org/10.1016/j.iswcr.2015.10.001>.
46. Fang, H.; Sun, L.; Tang, Z. Effects of rainfall and slope on runoff, soil erosion and rill development: an experimental study using two loess soils. *Hydrol. Process.* **2015**, *29*, 2649–2658. <https://doi.org/10.1002/hyp.10392>.
47. Han, D.; Deng, J.; Gu, C.; Mu, X.; Gao, P.; Gao, J. Effect of Shrub-Grass Vegetation Coverage and Slope Gradient on Runoff and Sediment Yield under Simulated Rainfall. *Int. J. Sediment Res.* **2021**, *36*, 29–37. <https://doi.org/10.1016/j.ijsrc.2020.05.004>.

48. Puigdefábregas, J. The Role of Vegetation Patterns in Structuring Runoff and Sediment Fluxes in Drylands: Vegetation and Sediment Fluxes. *Earth Surf. Process. Landf.* **2005**, *30*, 133–147. <https://doi.org/10.1002/esp.1181>.
49. Saxena, D.K.; Harinder Uses of Bryophytes. *Reson* **2004**, *9*, 56–65. <https://doi.org/10.1007/BF02839221>.
50. Oishi, Y. Evaluation of the Water-Storage Capacity of Bryophytes along an Altitudinal Gradient from Temperate Forests to the Alpine Zone. *Forests* **2018**, *9*, 433. <https://doi.org/10.3390/f9070433>.
51. Ah-Peng, C.; Cardoso, A.W.; Flores, O.; West, A.; Wilding, N.; Strasberg, D.; Hedderson, T.A. The role of epiphytic bryophytes in interception, storage, and the regulated release of atmospheric moisture in a tropical montane cloud forest. *J. Hydrol.* **2017**, *548*, 665–673. <https://doi.org/10.1016/j.jhydrol.2017.03.043>.
52. Ziadat, F.M.; Taimah, A.Y. Effect of rainfall intensity, slope, land use and antecedent soil moisture on soil erosion in an arid environment. *Land Degrad. Dev.* **2013**, *24*, 582–590. <https://doi.org/10.1002/ldr.2239>.
53. Zhang, X.; Yu, G.Q.; Li, Z.B.; Li, P. Experimental Study on Slope Runoff, Erosion and Sediment under Different Vegetation Types. *Water Resour. Manag.* **2014**, *28*, 2415–2433. <https://doi.org/10.1007/s11269-014-0603-5>.
54. Kim, J.K.; Onda, Y.; Kim, M.S.; Yang, D.Y. Plot-Scale Study of Surface Runoff on Well-Covered Forest Floors under Different Canopy Species. *Quat. Int.* **2014**, *344*, 75–85. <https://doi.org/10.1016/j.quaint.2014.07.036>.
55. Guevara-Escobar, A.; Gonzalez-Sosa, E.; Ramos-Salinas, M.; Hernandez-Delgado, G.D. Experimental analysis of drainage and water storage of litter layers. *Hydrol. Earth Syst. Sci.* **2007**, *11*, 1703–1716. <https://doi.org/10.5194/hess-11-1703-2007.2007>.
56. Chamizo, S.; Cantón, Y.; Domingo, F.; Belnap, J. Evaporative losses from soils covered by physical and different types of biological soil crusts. *Hydrol. Process.* **2013**, *27*, 324–332. <https://doi.org/10.1002/hyp.8421>.
57. Rodríguez-Caballero, E.; Cantón, Y.; Chamizo, S.; Afana, A.; Solé-Benet, A. Effects of biological soil crusts on surface roughness and implications for runoff and erosion. *Geomorphology* **2012**, *145*, 81–89. <https://doi.org/10.1016/j.geomorph.2011.12.042>.
58. Liu, F.; Zhang, G.; Sun, L.; Wang, H.; Sun, L. Effects of biological soil crusts on soil detachment process by overland flow in the Loess Plateau of China. *Earth Surf. Process. Landf.* **2016**, *41*, 875–883. <https://doi.org/10.1002/esp.4213>.
59. Chamizo, S.; Cantón, Y.; Lázaro, R.; Solé-Benet, A.; Domingo, F. Crust Composition and Disturbance Drive Infiltration Through Biological Soil Crusts in Semiarid Ecosystems. *Ecosystems* **2012**, *15*, 148–161. <https://doi.org/10.1007/s10021-011-9499-6>.
60. Zhao, Y.; Xu, M. Runoff and soil loss from revegetated grasslands in the hilly Loess Plateau region, China: influence of biocrust patches and plant canopies. *J. Hydrol. Eng.* **2013**, *18*, 387–393. [https://doi.org/10.1061/\(ASCE\)HE.1943-5584.0000633](https://doi.org/10.1061/(ASCE)HE.1943-5584.0000633).
61. Tu, N.; Yan, Y.; Dai, Q.; Ren, Q.; Meng, W.; Zhu, L.; Cen, L. Soil-fixing and water-retaining effects of lithophytic mosses in typical habitats of karst rocky desertification areas. *Ecology* **2021**, *41*, 6203–6214. <https://doi.org/10.5846/stxb202006111520>.
62. Paradelo, R.; van Oort, F.; Barré, P.; Billiou, D.; Chenu, C. Soil Organic Matter Stabilization at the Pluri-Decadal Scale: Insight from Bare Fallow Soils with Contrasting Physicochemical Properties and Macrostructures. *Geoderma* **2016**, *275*, 48–54. <https://doi.org/10.1016/j.geoderma.2016.04.009>.
63. Sorochkina, K.; Velasco Ayuso, S.; Garcia-Pichel, F. Establishing Rates of Lateral Expansion of Cyanobacterial Biological Soil Crusts for Optimal Restoration. *Plant Soil* **2018**, *429*, 199–211. <https://doi.org/10.1007/s11104-018-3695-5>.